arXiv:cond-mat/0408492v1 [cond-mat.supr-con] 23 Aug 2004

# Magnetization and Spin-Diffusion of Liquid $^3$He in Aerogel

J.A.Sauls,[1,2] Yu. M. Bunkov,[1] E. Collin,[1] H. Godfrin,[1] and P. Sharma[2]

[1] *Centre de Recherches sur les Très Basses Températures, Centre National de la Recherche Scientifique, Laboratoire Associé à l'Université J. Fourier, BP 166, 38042 Grenoble Cedex 9, France*

[2] *Department of Physics & Astronomy, Northwestern University, Evanston, IL 60208*

(Dated: March 23, 2022)

We report theoretical calculations of the normal-state spin diffusion coefficient of $^3$He in aerogel, including both elastic and inelastic scattering of $^3$He quasiparticles, and compare these results with experimental data for $^3$He in 98% porous silica aerogel. This analysis provides a determination of the elastic mean free path within the aerogel. Measurements of the magnetization of the superfluid phase provide a test of the theory of pairbreaking and magnetic response of low-energy excitations in the "dirty" B-phase of $^3$He in aerogel. A consistent interpretation of the data for the spin-diffusion coefficient, magnetization and superfluid transition temperature is obtained by including correlation effects in the aerogel density.

## I. INTRODUCTION

A strongly correlated Fermi liquid in the presence of disorder is realized when $^3$He is introduced into highly porous silica aerogel. The effects of disorder on the phase diagram and low-temperature properties of superfluid $^3$He have been a subject of widespread current interest. The thermodynamic and transport properties of $^3$He in aerogel are strongly modified by the scattering of $^3$He quasiparticles off the low-density aerogel structure. Here we summarize theoretical calculations of the magnetization[1] and spin transport[2] in the normal and superfluid states of $^3$He in high-porosity aerogel. The theoretical results are compared with experimental measurements of the normal-state spin-diffusion coefficient and magnetic susceptibility of the superfluid phase over the temperature range $1\,\mathrm{mK} \lesssim T \lesssim 100\,\mathrm{mK}$.[3]

For 98% porosity the typical diameter of the silica strands is $\delta \simeq 3\,\mathrm{nm}$. The mean distance between strands is $\xi_a \simeq 40\,\mathrm{nm}$, which is large compared to the Fermi wavelength, $\lambda_f \sim 0.1\,\mathrm{nm}$, but comparable to or less than the bulk coherence length, $\xi_0 = \hbar v_f/2\pi T_{c0} \simeq 20 - 80\,\mathrm{nm}$ over the pressure range $p = 34 - 0\,\mathrm{bar}$. The aerogel does not modify the bulk properties of normal $^3$He, beyond the formation of a couple of atomic layers of solid-like $^3$He adsorbed on the silica strands. The main effect of the aerogel structure is to scatter $^3$He quasiparticles moving with the Fermi velocity. At temperatures below $T^* \approx 10\,\mathrm{mK}$ elastic scattering by the aerogel dominates inelastic quasiparticle-quasiparticle collisions.[4] This limits the mean free path of normal $^3$He quasiparticles to $\ell \simeq 130 - 180\,\mathrm{nm}$ for aerogels with 98% porosity. (Note that there are variations in mean free path and correlation length for different aerogels with the same porosity.) Thus, the low-temperature limit for the spin diffusion coefficient is determined by elastic scattering from the aerogel. Comparison with experimental measurements for $T \ll T^*$ provides a determination of the transport mean free path due to scattering of quasiparticles by the aerogel.

Scattering by the aerogel also has dramatic effects on the formation and properties of the superfluid phases. If the coherence length (pair size) is sufficiently long compared to the typical distance between scattering centers, then the aerogel is well described by a homogeneous, isotropic scattering medium (HSM) with a mean-free path determined by the aerogel density. However, more elaborate scattering models are required if aerogel density correlations develop on length scales that are comparable with the pair correlation length.[5] Density correlations are observed at wavevectors $q \gtrsim \pi/\xi_a$ in the aerogel structure factor. We identify $\xi_a$ with the typical distance between silica strands or clusters, $\xi_a \approx 30 - 50\,\mathrm{nm}$ (c.f. Fig. 1). Figure 2 shows a comparison of the pair correlation length (Cooper pair size), $\xi = \hbar v_f/2\pi T_c$, as a function of pressure for $^3$He in aerogel, as well as that for pure $^3$He ($\xi_0 = \hbar v_f/2\pi T_{c0}$), with an aerogel correlation length of $\xi_a = 40\,\mathrm{nm}$.

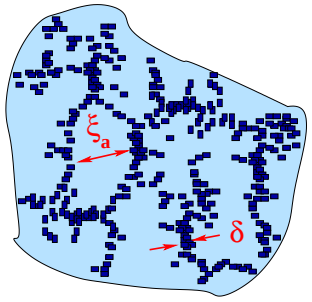



FIG. 1: A model silica aerogel showing low-density regions (light) of $^3$He surrounded by higher density strands and aggregates of silica (dark). The aerogel correlation length, $\xi_a \approx 30$ nm, is identified with the mean inter-strand distance. The aerogel strand diameter is approximately, $\delta \simeq 3$ nm.

The HSM provides a reasonable approximation to the properties of superfluid $^3$He-aerogel at low pressures; this model accounts semi-quantitatively for the reduction of $T_c$, including the critical pressure, $p_c$, and the pair-breaking suppression of the order parameter.[4,5] However, the HSM becomes a poorer description of $^3$He-aerogel at higher porosities and higher pressures where the pair size

is comparable to, or smaller than, the typical distance between scattering centers. This breakdown of the HSM is first evident in the quantitative discrepancies in the pressure dependence of $T_c$ particularly for higher porosity aerogels.[5,6]

The inhomogeneity of the aerogel on scales $\xi_a \gtrsim \xi$ leads to higher superfluid transition temperatures than predicted by the HSM with the same quasiparticle mean free path. Regions of lower aerogel density, of size of order $\xi_a$, are available for formation of the condensate. Thus, the qualitative picture is that of a random distribution of low density regions, 'voids', with a typical length scale, $\xi_a$, in an aerogel with a quasiparticle mean-free path, $\ell$. In the limit $\xi \sim \xi_a \ll \ell$, the superfluid transition is determined by the pairbreaking effects of dense regions surrounding the 'voids', and scales as $\delta T_c/T_{c0} \propto -(\xi/\xi_a)^2$. However, when the pair size is much larger than $\xi_a$ the aerogel is effectively homogeneous on the scale of the pairs and pairbreaking results from homogeneous scattering defined by the transport mean free path, which scales as $\delta T_c/T_{c0} \propto -(\xi/\ell)$. This latter limit is achieved at low pressures. Here we adopt a simplified version of the *inhomogeneous* scattering model[5] that incorporates correlations of the aerogel. The correlation effect is included by introducing an effective pairbreaking parameter that interpolates between these two limits: $x \to \tilde{x} = x/(1+\zeta_a^2/x)$, where $x = \xi/\ell$ and $\zeta_a \equiv \xi_a/\ell$. This heuristic treatment of aerogel correlations provides a good description of the pressure dependence of $T_c$ in zero field for $^3$He in aerogel over the whole pressure range.[7]

In section II we summarize experimental results for the magnetization of normal $^3$He in aerogel which are used to determine the amount and effect of the solid-like component of $^3$He that coats the aerogel strands. Section III describes NMR measurements of the spin diffusion coefficient of normal liquid $^3$He in aerogel and the theoretical calculations used to determine the elastic mean free path of quasiparticles. In p-wave superfluids quasiparticle scattering from the aerogel medium is intrinsically pairbreaking and leads to renormalization of nearly all properties of the superfluid phases. In section IV we summarize an analysis of the effects of scattering by the aerogel on the magnetic susceptibility based on the theoretical results for the disordered Balian-Werthamer (BW) phase,[1] modified to include the reduced pair-breaking effect of low-density regions of aerogel. The "dirty" B-phase is believed to describe the zero-field phase of superfluid $^3$He in aerogel, except in a narrow region near $T_c$.[8] The theory for the magnetization based on the "dirty" B-phase is tested against the measurements of the susceptibility.[3]

## II. MAGNETIZATION OF NORMAL $^3$HE

The nuclear magnetization, $M$, of normal liquid $^3$He at temperatures, $k_BT \ll E_f$, and fields, $\gamma\hbar H \ll E_f$, is given in terms of the (single-spin) quasiparticle density of states at the Fermi level, $N_f$, the nuclear gyromagnetic ratio for $^3$He, $\gamma$, and the exchange enhancement of the local field given in terms of the Landau interaction parameter, $F_0^a$, $\chi_N = M/H = 2N_f\mu^2/(1+F_0^a)$, where $\mu = \gamma\hbar/2$ is the nuclear magnetic moment of the $^3$He nucleus; $\chi_N$ is the nuclear spin susceptibility of the normal Fermi liquid.

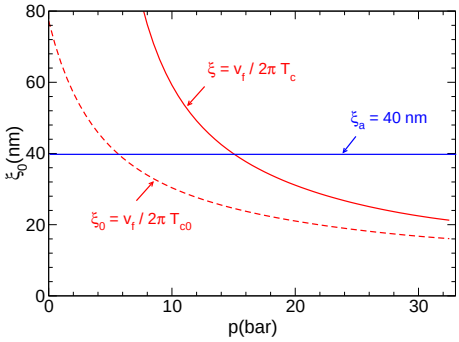



FIG. 2: The pair correlation length of superfluid $^3$He in aerogel (solid curve) as a function of pressure is shown in comparison with an aerogel strand-strand correlation length, $\xi_a \simeq 40\,$nm. A cross-over occurs near $p \approx 15\,$bar. The bulk $^3$He correlation length is also shown (dashed curve).

The effect of the aerogel on the magnetization of the normal *liquid* phase of $^3$He is expected to negligible. However, the aerogel structure is known to be covered with one or two layers of localized $^3$He atoms. These surface layers contribute a Curie-like susceptibility that obscures the Fermi-liquid contribution at low temperatures.[9] The surface contribution can be suppressed by the addition of $^4$He which preferentially plates the aerogel structure. The net effect is two-fold: (1) the surface Curie susceptibility is suppressed and (2) spin-spin scattering between $^3$He quasiparticles and the surface spins is suppressed. The cross-section of the aerogel may also be modified by $^4$He pre-plating, but we expect this effect to be relatively small.

We have performed accurate measurements of the magnetic susceptibility of normal liquid $^3$He in aerogel, with and without $^4$He pre-plating, using CW NMR at a field of $H = 37.3$ mT over a wide range of pressures and temperatures from $T \simeq 1$ mK up to a few hundred mK. The temperature was measured using the vibrating wire technique described in Ref. 10. The high temperature regime was calibrated against the Fermi temperature, $T_F$, and the melting curve thermometer. In Fig. 3 we show the magnetization data as a function of temperature for several pressures. The data is fit to a two-component form for the susceptibility; a Curie-Weiss term to describe the solid susceptibility with ferromagnetic correlations plus a temperature-independent term for the bulk Fermi liquid, $\chi = C/(T-\Theta_{\rm w})+\chi_{\rm N}$. The fit allows us to determine the ratio of the number of solid to liquid $^3$He atoms as a function of pressure, as well as the Curie-Weiss temperature of the solid spins. Pressurizing $^3$He in aerogel leads to increased solidification of $^3$He atoms, as shown in Fig. 4

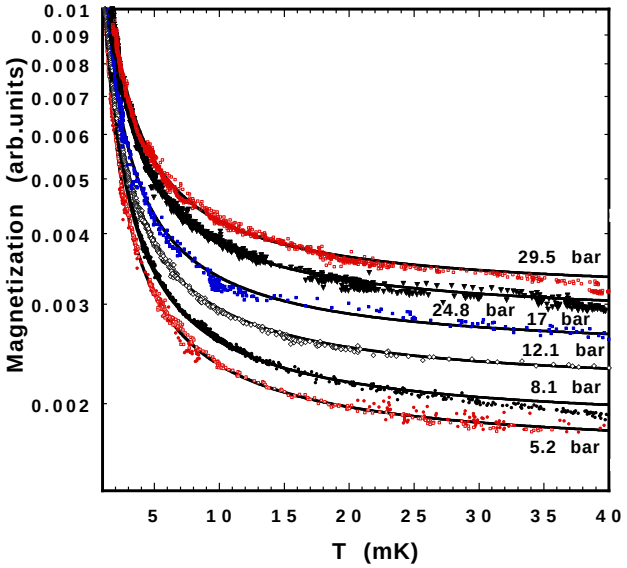



FIG. 3: The total magnetization of $^3$He in aerogel, both liquid and solid, for several pressures.

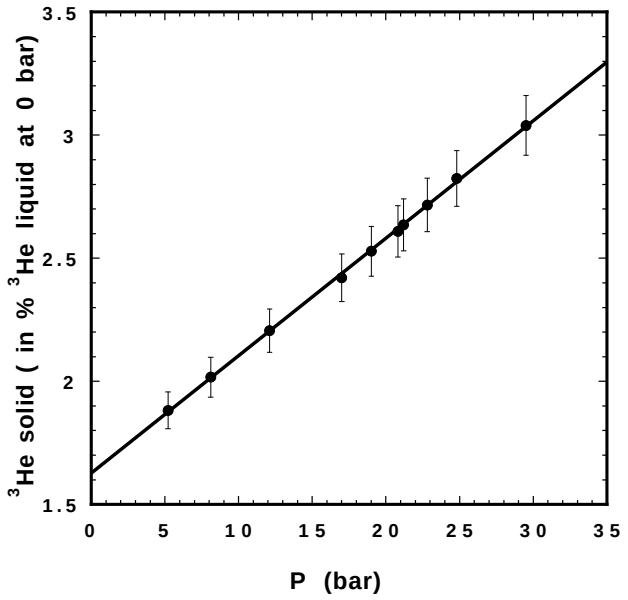



FIG. 4: The density of solid $^3$He atoms, normalized by density of liquid $^3$He for $p = 0$ bar.

and a decrease in the Curie-Weiss temperature as shown in Fig. 5. Both effects are well understood from previous studies on $^3$He adsorbed on homogeneous substrates (e.g. graphite) or heterogeneous substrates (powders, Vycor, etc.).[11,12] These results allow us to remove the contribution to the susceptibility from solid $^3$He, and thus, to extract the susceptibility of liquid $^3$He below superfluid transition.

We also performed measurements of the susceptibility of $^3$He in aerogel by pre-plating with $^4$He atoms. We added a small amount of $^4$He at a temperature of about 3 K and then cooled down. The solid $^3$He susceptibility

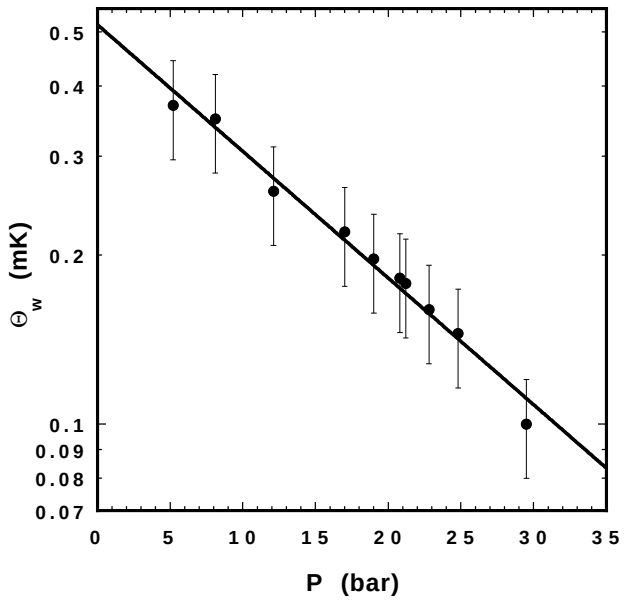



FIG. 5: The Curie-Weiss temperature, $\Theta_{\rm W}$, as function of pressure. The decrease reflects the increased average density of the solid layer in equilibrium with liquid $^3$He as the pressure increases.

is used to measure the amount of $^4$He adsorbed on the aerogel strands. The Curie-Weiss temperature is found to decrease in proportion to the amount of residual solid $^3$He.

For the NMR experiments reported here the solid and liquid components of $^3$He in aerogel exhibit a common NMR line, and are in the limit of "fast exchange" with a resonance frequency determined by the weighted average of the liquid and solid resonance frequencies, $\langle\omega\rangle = (M_{\rm liquid}\,\omega_{\rm liquid} + M_{\rm solid}\,\omega_{\rm solid})\,/\,(M_{\rm liquid} + M_{\rm solid})$.[9] We have performed the measurement of first and second moments of the NMR line, with and without $^4$He pre-plating. The NMR line is broadened by the presence of solid $^3$He by as much as 12 $\mu$Tesla, and the broadening scales by the ratio of the solid to liquid magnetization.

These experiments combined with NMR measurements of the spin-diffusion process in a field gradient provide a detailed characterization of the magnetic properties of solid and liquid $^3$He in the aerogel sample. The determination of the solid $^3$He magnetization, and the extrapolation of the Curie-Weiss behavior to temperatures below the superfluid transition allow us to extract the liquid component of the susceptibility in the superfluid phase of $^3$He in aerogel. Measurements of the spin-diffusion coefficient in the normal phase of $^3$He provide a measurement of the transport mean free path in aerogel.

## III. SPIN DIFFUSION

Measurements of the spin-diffusion coefficient for $^3$He in 98% aerogel were performed with small amounts of

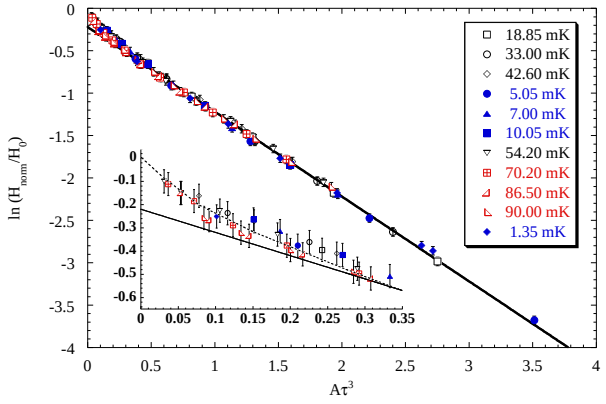



FIG. 6: The $\tau^3$ decay of the echo signal in a magnetic field gradient for $p = 0.5$ bar. The temperature range is from $T = 1$ to 90 mK. The coefficient, $A$, determined from the fit at a fixed temperature is related to the spin-diffusion coefficient and field gradient. The inset shows the short time, fast relaxation of unknown origin.

$^4$He added in order to displace the solid $^3$He. At $p = 0$ bar we see no signature of solid $^3$He, while at $p = 29.5$ bar we observe a small fraction ($\approx 0.25\%$ in the units of Fig. 4) of solid $^3$He.

We have used the typical spin echo sequences, $\pi/2-\tau-\pi$ and $\pi/2-\tau-\pi/2$, to measure the decay of echo signal as a function of time delay $\tau$ at a magnetic field gradient $G_z = 23\mu$T/cm. The solution of the Bloch equations for the spin echo signal in the magnetic field gradient reads is given by $H = H_\circ \exp(-2\tau/T_2 - A\tau^3)$, where $A = \frac{2}{3}\mathrm{D_M}(\gamma G_z)^2$. The decay of the spin echo is shown in Fig. 6 as function of $A\tau^3$ for our experimental conditions. On short time scales we observe small deviations from the $\tau^3$ dependence. These deviations are indicative of a fast relaxation mechanism of unknown origin. However, the main feature of the data is the $\tau^3$ dependence due to spin diffusion in a magnetic field gradient. The echo decay thus provides a direct measure of the spin diffusion coefficient of $^3$He in aerogel.

In pure $^3$He, the transport of magnetization in the hydrodynamic limit is given by the magnetization current density,

$$\mathbf{j}_i = -\mathrm{D_M}\,\boldsymbol{\nabla}\, M_i \tag{1}$$

where $M_i$ is the $i^{\rm th}$ component of the local magnetization, $\mathbf{M}(\mathbf{r}, t)$, and $\mathrm{D_M}$ is the spin diffusion coefficient. The hydrodynamic coefficient can be calculated from a kinetic theory of quasiparticles, which in the case of $^3$He in aerogel is the Landau-Boltzmann transport equation with the collision integral determined by both elastic scattering from the aerogel medium and inelastic quasiparticle collisions, i.e. binary collisions of quasiparticles within the narrow energy shell of order $k_BT$ near the Fermi surface. The general solution has the form,

$$\mathrm{D_M} = \frac{1}{3}v_f^2(1 + F_0^a)\tau_{\rm D}\,, \tag{2}$$

in the hydrodynamic limit, $\omega_{\rm L} \ll \tau_{\rm D}^{-1}$, where $\omega_{\rm L} = \gamma H$ is the Larmor frequency, $\tau_{\rm D}^{-1}$ is the collision rate that limits the transport of magnetization, $v_f$ is the Fermi velocity and $F_0^a$ is the $l = 0$ exchange interaction for $^3$He quasiparticles. The collision rate is calculated from the solution of the Landau-Boltzmann transport equation including both scattering channels.[13] The result of this calculation is summarized below.

At high temperatures ($T \gg T^*$) inelastic binary collisions of quasiparticle limit the transport of spin. The diffusion time approaches the bulk transport time,[14]

$$\tau_{\rm D} \to \tau_{\rm D}^{\rm bulk} = \frac{2\tau_{\rm in}}{\pi^2}\sum_{\nu=1}^{\rm odd}\frac{(2\nu+1)}{\nu(\nu+1)[\nu(\nu+1)-2\lambda_D]}\,, \tag{3}$$

where the inelastic quasiparticle lifetime is given by

$$\tau_{\rm in}^{-1} = \frac{N_f^2}{2p_f v_f}\langle W\rangle\, T^2\,, \tag{4}$$

with $N_f$ the single-spin density of states at the Fermi energy, and $W$ the binary collision probability for quasiparticles on the Fermi surface with momenta, $|\mathbf{p}_i| = p_f$. The Fermi-surface average is defined by

$$\langle W\rangle = \int \frac{d\Omega}{4\pi}\,\frac{W(\theta,\phi)}{2\cos(\theta/2)} \tag{5}$$

where $W(\theta,\phi)$ is the scattering probability for binary collisions of quasiparticles on the Fermi surface, defined in terms of the standard scattering angles.[15] The parameter $\lambda_D$ is given by the following average of the spin-flip scattering rate,

$$\lambda_D = 1 - \frac{1}{\langle W\rangle}\int\frac{d\Omega}{4\pi}\,\frac{W_{\uparrow\downarrow}\,(1-\cos\theta)\,(1-\cos\phi)}{4\cos(\theta/2)}\,. \tag{6}$$

However, at sufficiently low temperatures the scattering rate is limited by the quasiparticle collisions with the aerogel medium. Hence, as the temperature is reduced, the diffusion coefficient crosses over from a clean-limit behavior, $\mathrm{D_M} \propto T^{-2}$, to an impurity-dominated regime in which the diffusion coefficient approaches a temperature-independent value given by

$$\tau_{\rm D} \to \tau_{\rm el} = \ell/v_f\,, \quad T \ll T^*\,, \tag{7}$$

where $\ell$ is the limiting mean-free path for quasiparticles propagating ballistically through $^3$He then scattering elastically off the aerogel structure. This is the geometric mean free path for classical (point) particles, i.e. quasiparticles, travelling through the aerogel medium.

At intermediate temperatures the temperature dependence of the diffusion time is determined by both scattering channels. The solution to the Landau-Boltzmann transport equation[13] gives,

$$\tau_{\rm D} = \frac{\tau_{\rm in}}{4\pi^2}\sum_{N=0}^{\rm even}\frac{1}{1-\lambda_D/\alpha_N}\times \left\{\sum_{l=0,2,\ldots}^{N} d_l\,\beta(\gamma+\frac{1}{2};\frac{l+1}{2})\right\}^2\,, \tag{8}$$

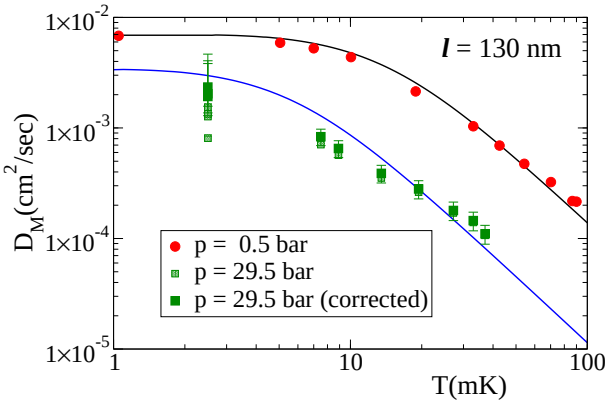



FIG. 7: Comparison to our experimental data.[3] We fit the inelastic scattering amplitude to the high-temperature data and obtain good agreement for a mean free path $\ell = 130$ nm for the entire temperature range.

where $\alpha_N = (\gamma+N)(1+2\gamma)+\frac{N(N-1)}{2}$, the Beta function, $\beta(\mu;\nu) = \Gamma(\mu)\Gamma(\nu)/\Gamma(\mu+\nu)$, is related to the standard Gamma function,[16] and

$$\gamma = \frac{1}{2}\sqrt{1+\frac{1}{\pi^2}\frac{\tau_{\rm in}}{\tau_{\rm el}}}\,, \tag{9}$$

is the dimensionless parameter that controls the cross-over from elastic- to inelastic-dominated scattering. The coefficients in Eq.(8) are obtained from the recursion relation,

$$d_{l+2} = \frac{l(l-1)+2l(1+2\gamma)-2\alpha_N+2\gamma+4\gamma^2}{(l+2)(l+1)}\,d_l\,, \tag{10}$$

and the normalization condition

$$\begin{aligned} 1 \;=\; & \sum_{l=0,2,\ldots}^{N}\sum_{l'=0,2,\ldots}^{N} d_l\, d_{l'}\,, \times \\ & \Big\{2\gamma^2\,\beta(2\gamma;\tfrac{l+l'+1}{2}) + 2\gamma^2\,\beta(2\gamma;\tfrac{l+l'+3}{2}) - \\ & 2\gamma l'\,\beta(2\gamma+1;\tfrac{l+l'+1}{2}) + \tfrac{1}{2}\,ll'\,\beta(2\gamma+2;\tfrac{l+l'-1}{2})\Big\}\,. \end{aligned} \tag{11}$$

The calculated spin diffusion coefficient is shown in Fig. 7 for $p = 0.5$ bar and for $p = 29.5$ bar. The spin-diffusion coefficient decreases as $\mathrm{D_M} \propto T^{-2}$ at high temperatures and coincides with the bulk measurements of the $^3$He spin-diffusion coefficient by Ref. 17. Thus, we fit the average binary quasiparticle collision probability, $\langle W\rangle$, at each pressure to the high-temperature diffusion coefficient with the spin-flip scattering rate parameter, $\lambda_{\rm D}$, obtained from the scattering model of Ref. 18. The bulk Fermi liquid parameters used in the calculation of $\mathrm{D_M}$ for $^3$He in aerogel are taken from Ref. 19.

The low-pressure results provide the best data set to compare with the theory. The theoretical result shown in Fig. 7 corresponds to a low-temperature (elastic) mean free path of $\ell = 130$ nm. Note that the cross-over from the high-temperature inelastic limit to the low-temperature aerogel-dominated regime is well described by the theory at low pressure.

The aerogel mean-free path is expected to be essentially pressure independent, so long as the integrity of the aerogel is not damaged under hydrostatic pressure. Thus, the calculation of the spin-diffusion coefficient is made with the same aerogel mean-free path and the bulk scattering parameters appropriate for $p = 29.5$ bar. The result is also shown in Fig. 7. The experimental data are consistent with the theoretical results within the estimated errors. The higher pressure spin-diffusion data is also shown corrected for the small, but measurable, component of solid magnetization that is transported by diffusion due fast exchange with the liquid. The main result of this analysis is the determination of the elastic mean free path. This parameter is relevant to the mechanism for pairbreaking, the low-energy excitation spectrum and polarizability of the superfluid phase of $^3$He in aerogel.

## IV. MAGNETIZATION OF $^3$HE-B-AEROGEL

Measurements of the B-like suppression of the susceptibility in $^3$He-aerogel have been reported for two or more monolayers of $^4$He added to displace the solid layer of $^3$He.[9,20] Experiments carried out in Grenoble[3] on pure $^3$He in aerogel also show the B-like suppression of the liquid component of the susceptibility, obtained by subtracting the Curie-Weiss component from the solid $^3$He coating the aerogel strands. In the following we compare theoretical results for the magnetic susceptibility of the "dirty B phase" of superfluid $^3$He with these recent experimental measurements. The magnetization measurements in the superfluid phase were carried out on the same aerogel used in measurements of the spin echo decay. Thus, the transport mean free path of this aerogel, $\ell = 130$ nm, is known.

In the theoretical analysis of the magnetization we consider only elastic scattering of $^3$He quasiparticles off the aerogel structure, and we neglect the spin-dependence of the scattering cross-section for $^3$He quasiparticles with by the polarized solid. The splitting of the cross-section by the polarized solid is expected to be a very small effect which is unimportant in calculating pair-breaking effects, except in a very narrow temperature interval corresponding to the $A_1$-$A_2$ transition.[7]

The nuclear spin susceptibility of pure superfluid $^3$He-B agrees quantitatively to leading order in $T_c/E_f$ with the result of Ref. 21 for the susceptibility of the Balian-Werthamer state,

$$\chi_B/\chi_N = \frac{(1+F_0^a)\left[\frac{2}{3}+Y(\frac{1}{3}+\frac{1}{5}F_2^a)\right]}{1+F_0^a(\frac{2}{3}+\frac{1}{3}Y)+\frac{1}{5}F_2^a(\frac{1}{3}+\frac{2}{3}Y)+\frac{1}{5}F_2^aF_0^aY}\,, \tag{12}$$

where $Y(T)$ is the well-known Yosida function,

$$Y(T) = 1-\pi T\sum_{\varepsilon_n}\frac{\Delta^2}{[\varepsilon_n^2+\Delta^2]^{3/2}}\,, \tag{13}$$

$\Delta(T)$ is the B-phase gap amplitude, and $F_2^a$ is the $l = 2$ harmonic of the exchange interaction.

For a B-like phase of $^3$He in aerogel depairing of the $S_z = 0$ Cooper pairs by scattering from the aerogel leads to sizeable changes in the magnetization. In addition to the suppression of $T_c$ relative to $T_{c0}$, the magnitude of the susceptibility, particularly at low temperatures, is sensitive to the density of quasiparticle states below the gap, $\varepsilon < \Delta$, produced by pairbreaking.

In the HSM model, for either Born or unitarity scattering, the generic form of Eq. (12) for the B-phase susceptibility is preserved with the replacement of the gap and Yosida functions by impurity-renormalized gap and response functions.[1,22] The results can be summarized by Eq. (12) with the replacement of $Y(T) \to \tilde{Y}(T)$. For example, in the unitary scattering limit,

$$\tilde{Y} \;=\; 1 - \pi T \sum_n \frac{\Delta^2}{[\tilde{\varepsilon}_n^2 + \Delta^2]^{3/2}} \left\{ \frac{1}{1 + \frac{1}{3}\left(\frac{1}{\tilde{\varepsilon}_n}\right)^2 \frac{\Gamma_N \Delta^2}{\sqrt{\tilde{\varepsilon}_n^2 + \Delta^2}}} \right\}, \quad (14)$$

where $\Gamma_N$ is related to the aerogel mean-free path for normal-state $^3$He quasiparticles

$$\Gamma_N = \frac{\hbar v_f}{2\ell}\,. \quad (15)$$

The gap equation and renormalized Matsubara frequencies are given by

$$\ln(T/T_{c0}) = \pi T \sum_n \left( \frac{1}{\sqrt{\tilde{\varepsilon}_n^2 + \Delta^2}} - \frac{1}{|\varepsilon_n|} \right), \quad (16)$$

$$\tilde{\varepsilon}_n = \varepsilon_n + \Gamma_N \tilde{\varepsilon}_n \sqrt{\tilde{\varepsilon}_n^2 + \Delta^2}/\tilde{\varepsilon}_n\,, \quad (17)$$

with $\varepsilon_n = (2n+1)\pi T$. In the HSM model the gap and excitation spectrum are determined by the mean free path, $\ell$. Pairbreaking occurs homogeneously throughout the liquid. The dimensionless pairbreaking parameter that determines $T_c$ is given by the ratio, $x_c = \Gamma_N/2\pi T_c$. At lower temperatures the pairbreaking parameter that enters the gap equation and renormalized Matsubara frequencies scales as $x = \Gamma_N/2\pi T$. Detailed discussion of the results for the magnetization within the HSM are given in Refs. 1,22.

When the inhomogeneities of the aerogel occur on length scales comparable to or greater than the pair correlation length the HSM model overestimates the magnitude of pairbreaking. For a fixed mean free path this aerogel correlation effect leads to an increase in $T_c$, and to a reduction in the number of low-energy excitations produced by scattering within the aerogel. We introduce the effective pairbreaking parameter for the gap and excitation spectrum based on a similar scaling procedure introduced for the transition temperature.[7] For $T_c$ the effective pairbreaking parameter, $\tilde{x}_c = x_c/(1 + \zeta_a^2/x_c)$, interpolates between the HSM model with $\tilde{x}_c \propto -(\xi/\ell)$ valid for $\xi \gg \xi_a$ and the inhomogeneous limit with $\tilde{x}_c \propto -(\xi/\xi_a)^2$ valid for $\xi \ll \xi_a$. At lower temperatures the scaling is given by $\tilde{x} = x/(1+\zeta_a^2/x_c)$, which coincides with $\tilde{x}_c$ for $T \to T_c$, and accounts for the corresponding reduction in the pairbreaking density of states at temperatures, $T \ll T_c$. Replacing the pairbreaking parameter of the HSM by the effective pairbreaking parameter leads to a modification of the low-energy excitation spectrum and magnetization. Physical properties that are not spatially resolved on the scale of $\xi_a$ should be well described by this approach.

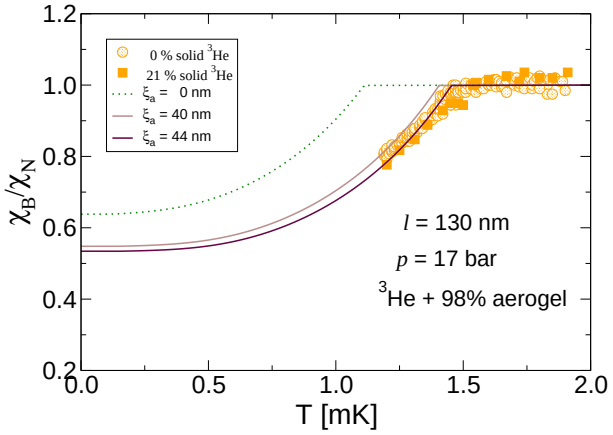



FIG. 8: Comparison to experimental data for the magnetic susceptibility at $p = 17$ bar. Only the liquid contribution to the susceptibility is plotted for the two measurements with different amounts of solid $^3$He. The theoretical calculation is based on the HSM and the dirty BW phase.

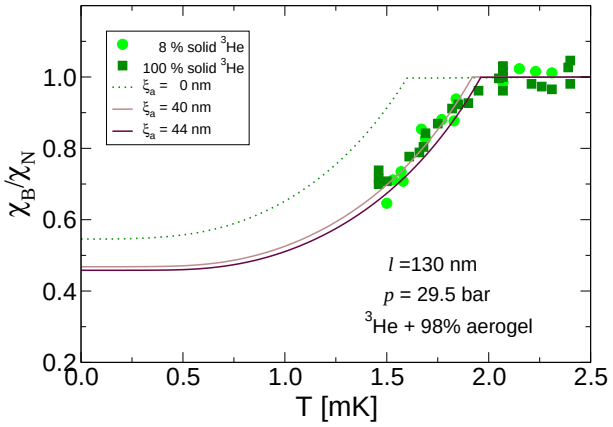



FIG. 9: Comparison to experimental data for the magnetic susceptibility at $p = 29.5$ bar. Only the liquid contribution to the susceptibility is plotted for the two measurements with different amounts of solid $^3$He. The theoretical calculation is based on the HSM and the dirty BW phase.

The magnetization of superfluid $^3$He in $\approx 98\%$ aerogel was measured by NMR in pure $^3$He in aerogel and with varying amounts of $^4$He pre-plating, and for intermediate ($p = 17.0$ bar) and high ($p = 29.5$ bar) pressures. We use the analysis of the normal $^3$He susceptibility (shown in Fig. 3) to subtract the solid $^3$He component. In this pressure range the effects of inhomogeneity in the aerogel are clearly reflected in the weaker suppression of $T_c$ compared to the relative suppression at lower pressures.[7]

Figures 8 and 9 show results for the magnetic susceptibility of the "dirty" B-phase calculated for a mean free path of $\ell = 130\,\mathrm{nm}$. As is clearly shown $T_c$ as predicted by the HSM model (i.e. $\xi_a = 0$) is too strongly suppressed. In addition the HSM predicts a larger increase in the spin susceptibility for $T \to 0$, indicative of an overestimate of the density of polarizable low-energy quasiparticles.

The effect of aerogel correlations, corresponding to typical void sizes of $\xi_a \approx 40-44\,\mathrm{nm}$, is shown in both figures. The correlations lead to weaker suppression of $T_c$ compared to the HSM model and to reduced pairbreaking. Both effects are clearly seen in the data for both pressures, and are consistent with one another and with the mean free path determined from the spin-diffusion data.


[1] P. Sharma and J. A. Sauls, J. Low Temp. Phys. **125**, 115 (2001).
[2] P. Sharma, Ph.D. thesis, Northwestern University (2003).
[3] E. Collin, Ph.D. thesis, Université Joseph Fourier, Grenoble (2002).
[4] D. Rainer and J. A. Sauls, J. Low Temp. Phys. **110**, 525 (1998).
[5] E. V. Thuneberg, S.-K. Yip, M. Fogelström, and J. A. Sauls, Phys. Rev. Lett. **80**, 2861 (1998).
[6] G. Lawes, S. Kingsley, N. Mulders, and J. M. Parpia, Phys. Rev. Lett. **84**, 4148 (2000).
[7] J. A. Sauls and P. Sharma, Phys. Rev. B **68**, 224502 (2003).
[8] G. Gervais, K. Yawata, N. Mulders, and W. P. Halperin, Phys. Rev. B **66**, 054528 (2002).
[9] D. Sprague, T. Haard, J. Kycia, M. Rand, Y. Lee, P. Hamot, and W. Halperin, Phys. Rev. Lett. **75**, 661 (1995).
[10] C. Winkelmann, E. Collin, Y. M. Bunkov, and H. Godfrin, J. Low Temp. Phys. **135**, 3 (2004).
[11] H. Godfrin and R. E. Rapp, Advan. Phys. **44**, 113 (1995).
[12] A. Golov and F. Pobell, Phys. Rev. B **53**, 12647 (1996).
[13] P. Sharma and J. A. Sauls, Physica **B 284-288**, 297 (2000).
[14] G. A. Brooker and J. Sykes, Phys. Rev. Lett. **21**, 279 (1968).
[15] G. Baym and C. J. Pethick, *Landau Fermi-Liquid Theory* (Wiley, New York, 1991).
[16] M. Abramowitz and I. A. Stegun, *Handbook of Mathematical Functions* (Dover, New York, 1970).
[17] A. C. Anderson, W. Reese, and J. C. Wheatley, Phys. Rev. **127**, 671 (1962).
[18] J. A. Sauls and J. W. Serene, Phys. Rev. **B24**, 183 (1981).
[19] W. P. Halperin and E. Varoquaux, in *Helium Three*, edited by W. P. Halperin and L. P. Pitaevskii (Elsevier Science Publishers, Amsterdam, 1990), p. 353.
[20] B. I. Barker, Y. Lee, L. Polukhina, D. D.Osheroff, L. W. Hrubesh, and J. F. Poco, Phys. Rev. Lett. **85**, 2148 (2000).
[21] J. W. Serene and D. Rainer, Phys. Rep. **101**, 221 (1983).
[22] V. P. Mineev and P. L. Krotkov, Phys. Rev. B **65**, 024501:10pp (2002).